Journal of ELECTRONIC MATERIALS, Vol. 47, No. 7, 2018
https://doi.org/10.1007/s11664-018-6231-8

Synthesis and Characterization of Cross-Linked Nanocomposite as a Gate Dielectric for *p*-Type Silicon Field-Effect Transistor

ADELEH HASHEMI,[1] ALI BAHARI,[1,3] and SHAHRAM GHASEMI[2]

1.—Department of Solid State Physics, University of Mazandaran, Babolsar 4741695447, Iran. 2.—Faculty of Chemistry, University of Mazandaran, Babolsar, Iran. 3.—e-mail: a.bahari@umz.ac.ir

A good cross-linking between a povidone–silicon oxide nanocomposite has been created using a polar solvent. Furthermore, the effect of annealing temperatures (150°C, 200°C, and 240°C) on the solution-processed povidone–silicon oxide dielectric films has been studied. Fourier transform infrared spectroscopy and x-ray photoelectron spectroscopy were applied to identify the chemical interactions of the nanocomposite. Morphology of the thin films was examined using atomic force microscopy. Electrical parameters of field effect transistors (FETs) were calculated on the basis of the information obtained from current–voltage (*I*–*V*) and capacitance–voltage (*C*–*V*) measurements in the metal–insulator–semiconductor structure. Nanocomposite films had very low surface roughness (0.036–0.084 nm). Si-O-Si and Si-O-C covalent bonds as well as Si-OH hydrogen bonds were formed in the nanocomposite structure. High hole mobilities (1.15–3.87 $cm^2\ V^{-1}\ s^{-1}$) and low leakage current densities were obtained for the *p*-type Si FETs. The decrease in the Si-OH hydrogen bonds in the dielectric film annealed at 150°C led to a decrease in capacitance and leakage current as well as threshold voltage, and resulted in an increase in mobility and on/off current ratio. By further increasing the annealing temperatures (200°C and 240°C), the binding energies of all the bonds were shifted toward lower values. Therefore, it was concluded that many bonds could have degraded and that defects might have formed in the dielectric film nanostructure leading to a decline in the electrical parameters of the FETs.

Key words: *p*-Type Si FET, gate dielectric, annealing temperature, leakage current, charge carrier mobility

INTRODUCTION

Silicon oxide as a gate dielectric has been widely used in field-effect transistors (FET) during the last four decades.[1–5] Electron mobilities up to 150 $cm^2\ V^{-1}\ s^{-1}$ and hole mobilities up to 10 $cm^2\ V^{-1}\ s^{-1}$ have been reported for silicon oxide gate dielectric films.[6,7] One disadvantage of oxide silicon dielectric thin films is the high leakage current.[2,8,9] The leakage current densities have been recorded from 10^{-7} A/cm^2 to 10^{-2} A/cm^2 at the gate voltage between 0 and − 2.5 V f or an l/SiO_2/*p*-type Si structure.[10] In addition, these devices are often made using vacuum deposition methods such as chemical vapor deposition (CVD) and physical vapor deposition, which require long pump-down times and increased fabrication costs.[1,11,12]

Thus, organic materials have been extensively studied by many researchers.[13–17] Polymeric thin films can be deposited by solution deposition methods at room temperature in a few seconds without using vacuum equipment,[13–15] so they are suitable for large-area fabrication at a lower cost.[13–15]

(Received January 23, 2017; accepted March 14, 2018; published online March 28, 2018)

The polymeric materials as gate dielectrics also provide a smooth surface and low leakage current.[18,19] Bao et al.,[11] reported root-mean-square (rms) roughness of 0.2 nm for pentacen dielectric film grown on silicon oxide. They also reported a roughness of 1.5 nm for silicon oxide dielectric film deposited by CVD.[11] A poly (3-hexylthiophene) (P3HT)-organic FET based on poly (4-vinylphenol)–poly (melamine-co-formaldehyde) dielectric film (with rms roughness of 0.28 nm) spin-coated demonstrated hole mobility of 0.06 $cm^2\ V^{-1}\ s^{-1}$.[20] The hole mobility of 0.62 $cm^2\ V^{-1}\ s^{-1}$ was recorded for a FET based on poly (vinyl alcohol) (CR-V) dielectric film (with rms roughness of 0.31 nm) spin-coated on Si substrate.[21] It is well known that polaron carriers in polymers result in a decrease in the charge carrier mobility ($< 1\ cm^2\ V^{-1}\ s^{-1}$).[13,14,22]

In order to improve the performance of the FETs, the use of organic and inorganic composites as gate dielectrics have recently received much attention.[5,8,18,23–26] Lee et al.,[12] reported rms roughness of 0.45 nm, high hole mobility of 2.5 $cm^2\ V^{-1}\ s^{-1}$ and low leakage current (about 10^{-8} A/cm^2 at 2 MV cm^{-1}) for a silicon oxide–polysiloxan composite dielectric film deposited by spin coating. However, it is important to create a strong connection between the organic and inorganic phases through hydrogen or covalent bonds. One way to enhance the compatibility between the two phases is by using silane coupling agents (cross-liking agents) which improve the interfacial interactions and connect the polymer chains to inorganic nanoparticles. This prevents inorganic nanoparticle aggregation and forms a smooth surface.[27,28] Leakage current densities have been reported from 10^{-5} A/cm^2 to 10^{-8} A/cm^2 at gate voltages between − 20 V and 20 V for a polymethyl methacrylate (PMMA)–silicon oxide nanocomposite which was synthesized using a silane coupling agent.[28,29] Selecting a suitable solvent also creates a good cross-linking and reduces the leakage current.[11,21,30,31] Furthermore, the annealing temperature has a great effect on the thin film nanostructure.[4,32–34]

The present study was aimed to obtain strong interactions and a homogeneous dielectric film with a smooth surface by applying a high-k solvent and a silane coupling agent. In order to achieve the goals, we synthesized a povidone–silicon oxide nanocomposite using a coupling agent through the sol–gel process. The solution was then spin-coated onto *p*-type silicon (100) substrates. The films were annealed at 150°C, 200°C, and 240°C, and the effects of these annealing temperatures on the nanostructure of the films and their compatibility with *p*-type silicon semiconductors were investigated.

EXPERIMENTAL

Nanocomposite Synthesis

Tetraethyl orthosillicate (TEOS; 99.999% Aldrich) as the silicon oxide precursor, povidone (average mol wt 40,000 Aldrich) as the polymeric material and trimethoxysilyl propyl metacrylate (97%; Merck) as the silane coupling agent were used in this experiment. The povidone–silicon oxide nanocomposite was synthesized using the sol–gel method. For this, 0.1 g povidone was dissolved in 10 ml ethanol (ETOH; 99.99%; Merck). 44.68 ml deionized water and 0.5 ml of 0.4 M hydrogen chloride (Hcl) were applied to dissolve 10.87 g TEOS and 0.48 ml trimethoxysilyl propyl metacrylate. Then, the three solutions were mixed in the molar ratio of 1:1:0.05 (povidone:TEOS:trimethoxysilyl propyl metacrylate) at 400 rpm and at 70°C. The obtained homogeneous gel was dried at 70°C so that the watery substance could be removed.[9] The powder obtained from polymerization was dissolved in benzene alcohol solvent to obtained a solution of 20 mg/ml.

Preparation of Thin Films

Initially, *p*-type silicon (100) wafers were cut into pieces of 1 × 1 cm. They were then cleaned using acetone and ETOH and were put into ultrasonic cleaner containing ETOH for 30 min. The povidone–silicon oxide nanomomposite solution was deposited on the purified *p*-type Si (100) substrates by spin-coating at 7000 rpm for 15 s. Four films were deposited in a similar way and three of them were annealed at the following temperatures: 150°C, 200°C, and 240°C for 1 h.

RESULTS AND DISCUSSION

Nanocomposite Characterization

Fourier transforms infrared (FTIR) spectroscopy (a Bruker-Tensor 27 spectroscope) was used to ensure the outcome of polymerization of the sol–gel process. The FTIR spectra of the synthesized nanocomposite powder and pure povidone powder are presented in Fig. 1. Table I summarizes the bond characteristics. A comparison of the two spectra in Fig. 1 depicts many differences in the synthesized nanocomposite and pure povidone.

The first difference is the emergence of Si-OH and Si-O-Si bonds in the synthesized nanocomposite which is due to hydrolysis and condensation processes, respectively. Also, the intensity of the Si-O-Si bonds is stronger than Si-OH bonds (the second difference). This shows that the condensation process was performed well and that covalent bonds were formed between the coupling agent and the silicon dioxide.[35,36] The third difference relates to the presence of O-Si-C bonds which is due to the chemical interactions between the organic and inorganic phases. The fourth difference can be found in the peak of the carbon element of the synthesized material. The peak position of this element compared to that of the pure povidone is shifted to a lower wave number. Moreover, the intensity of peak decreases. The change in the wave number shows the formation of new bonds with

Table I. FTIR bonds assignment of pure povidone and povidone–silicon oxide nanocomposite

Bond characteristic	Wave number (Cm^{-1})	References	Bond characteristic	Wave number (Cm^{-1})	References
Povidone			Povidone–silicon oxide		
N-C=O	651	18, 27, 34	Si-O-Si	460	18, 27, 34
C-N	1074	18, 27, 34	N-C=O	566	18, 27, 34
C-H_2 Twist	1221	18, 27, 34	Si-O-Si stretching	800	18, 27, 34
C-N stretching	1292	18, 27, 34	Si-OH	962	18, 27, 34
C-H_2	1375	18	Si-O-Si stretching	1081	18, 27, 34
C-H_2 Scissor	1494-1497	18	O-Si-C	1108	18, 27, 34
C=O	1656	27, 34	C=O	1646	18, 27, 34
C-H_2 Stretchin	2959	18	C-H_2 stretching	2959	18, 27, 34
O-H	3427	18	O-H	3453	18, 27, 34

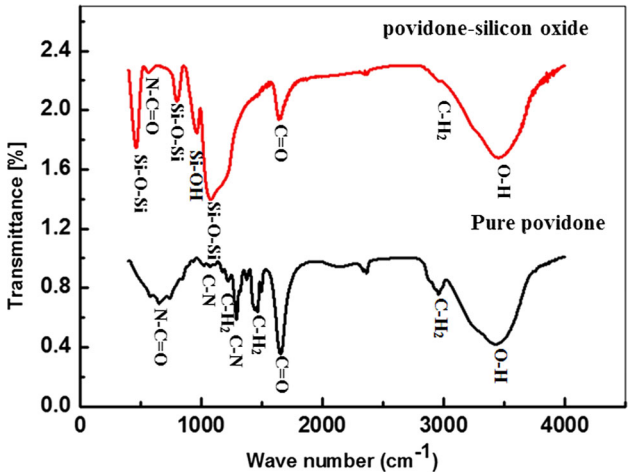

Fig. 1. FTIR spectra of pure povidone and povidone–silicon oxide nanocomposite.

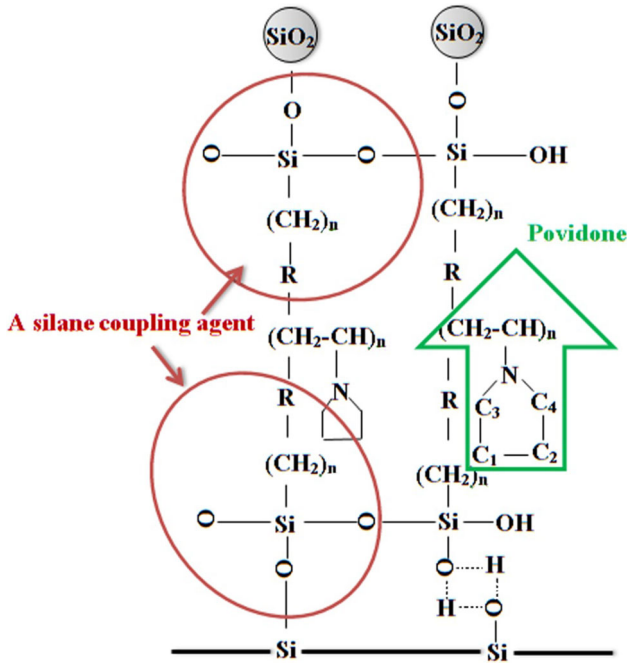

Fig. 2. Schematic illustration of the interactions between the povidone–silicon oxide nanocomposite and the *p*-type silicon substrate.

carbon elements. The reduction in the peak intensity of this element could be due to the lower percentage of carbon in the nanocomposite. The presence of four bonds of pure povidone (566 cm^{-1}, 1081 cm^{-1}, 1646 cm^{-1}, and 2960 cm^{-1}) in the synthesized nanocomposite indicates the existence of povidone organic material. Therefore, it can be concluded that the silane coupling agent formed chemical interactions between the silicon oxide nanoparticles and the povidone chains and the cross-linked povidone–silicon oxide nanocomposite was formed. A schematic illustration of the interactions between the nanocomposite elements and the *p*-type silicon substrate is shown in Fig. 2.

In order to study the interactions between the elements of the thin films, the narrow scan x-ray photoelectron spectroscopy (XPS) technique (with an Al-K_α x-ray source operated at 1400 eV) of the povidone–silicon oxide nanocomposite films was performed. The XPS spectra were deconvoluted by using a spectral data processor, *v*.4.4, software. The number and location of the peaks were considered in such a way that the best fit with the original spectrum could be obtained. The characteristics of the peaks were identified on the basis of the differences in the binding energy of bonds reported in several studies[37,39,40,49–52] Figure 3a and b shows deconvoluted XPS spectra of Si2p and O1 s electron orbitals of nanocomposite films annealed at various temperatures. Identification of deconvoluted XPS Si2p and C1s peaks in Fig. 3a and b and their corresponding chemical structure are presented in Table II. As Fig. 3 shows, in the spectrum of non-annealed nanocomposite films, the peaks of the two orbitals are asymmetrical and can be divided into several peaks. The presence of Si-OH (binding energy of 99.3 eV and intensity of 414.7) and Si-O-Si (binding energy of 98.4 eV and intensity of 416) bonds in Si2p electron orbital indicate that the organosilane groups of coupling agent were

Table II. Identification of the deconvoluted XPS Si2p and C1s peaks from Fig. 3a and b, and their corresponding chemical structure and intensity

Electron orbital	Bond characteristic	References	BE (eV) counts	Non-annealed	150°C	200°C	240°C
Si2p	Si-O-Si	37, 39, 49, 50	BE	98.4	98.1	97.35	97.65
			Cts	416	194.8	393.8	1010
	Si-OH	37, 49, 50	BE	99.3	98.8		
			Cts	414.7	89.9		
	SiO_3C	37, 49	BE	102.2	102.4	101.56	101.7
			Cts	62.8	34.5	55.8	179.9
	SiO_2	40, 49, 50	BE	103.4			
			Cts	38.8			
C1 s	O-Si-C	37, 40, 49	BE	283.12		283.3	283.24
			Cts	40.8		253	107.5
	C1	51	BE	284.6	284.6	284.4	284.22
			Cts	82.9	103	173.7	214.3
	C2	51	BE	285	285.3		
			Cts	59.2	118.3		
	C3	51	BE	285.8	286.3	285.8	285.85
			Cts	2.3	263	38	78.7
	C4	51	BE	287.5	287.8	287.5	285.85
			Cts	16.1	60.1	28.9	78.7

hydrolyzed and after condensation formed hydrogen bonds with OH groups of the substrate. In addition, the appearance of O-Si-C bonds in the C1s spectra is another proof which shows the occurrence of chemical interactions between the organic and inorganic elements of nanocomposite film.[35,36]

In the spectra obtained from the nanocomposite film annealed at 150°C, Si-O-Si bonds (98.1 eV) become dominant in Si2p orbitals and the intensity of Si-OH bonds reduced. This might have been caused by the temperature at which a lot of hydroxyl groups of Si-OH hydrogen bonds that existed in non-annealed film left the matter in the form of water and the stronger Si-O-Si covalent bonds were formed. The formation of Si-O-Si bonds indicates that good adhesion between the nanocomposite film elements and the *p*-type Si substrate is created (see Fig. 2). In addition, the values of the binding energy of Si-OH and Si-O-Si bonds in Si2p orbital shift to a lower binding energy compared to those of the non-annealed film (0.3 eV and 0.5 eV, respectively) (see Fig. 3a, b). Also, SiO_2 bonds that existed in the non-annealed film disappear. This suggests that more favorable interactions between the two phases have occurred. In the C1s orbital spectrum of this sample, the carbon peak linked with silicon (Si-O-C) disappears and the binding energy and intensity of other carbon elements have higher values (Fig. 3b). Since a change in binding energy is caused by changes in electron density,[37–40] it can be concluded that the interactions occurred at this temperature.

By increasing the annealing temperature to 200°C, Si-OH and Si-O-Si bonds of Si2p orbital disappear and a peak also appears at the binding energy which is c.1 eV less than that of the Si-O-Si bond. The binding energy of SiO_3C peak similarly shifts to lower binding energy (c.1 eV). The shift of around 1 eV could have been due to the loss of a bond with oxygen element or changes in the second neighbors.[37–40] Therefore, the peak appearing at the binding energy of 97.37 eV could be related to the Si-Si bonds. The fact that hydrogen Si-OH bonds did not appear at this temperature is probably due to the drying process being completed. O-Si-C bonds which were missing in the C1 s orbital at the previous temperature dominate the peaks in the orbital at this temperature. Changes also occur in the binding energy of carbons bonded with other elements. This is likely to be due to the film silicon atoms that were desorbed out of the substrate forming chemical interactions with themselves and with carbon atoms. So it could be inferred that aggregation occurred in the nanostructure of the film.

At the highest annealing temperature (240°C), small changes happen in the binding energy of bonds which may be related to physical phenomena caused by the changes in the film thickness and the length or angle of the bonds.[37–40] In addition, the intensity of the Si-Si bonds has greatly increased (from 393.8 in the film annealed at 200°C to 1010 in the film annealed at 240°C) while the intensity of the O-Si-C bonds has decreased (from 253 in the film annealed at 200°C to 107.5 in the film annealed at 240°C). This might have been caused by the degradation of the interactions between the silicon and carbon atoms of the film annealed at 240°C.

Morphology Studies

Figure 4 shows atomic force microscopy (AFM) images of povidone–silicon oxide nanocomposite films annealed at different temperatures. There

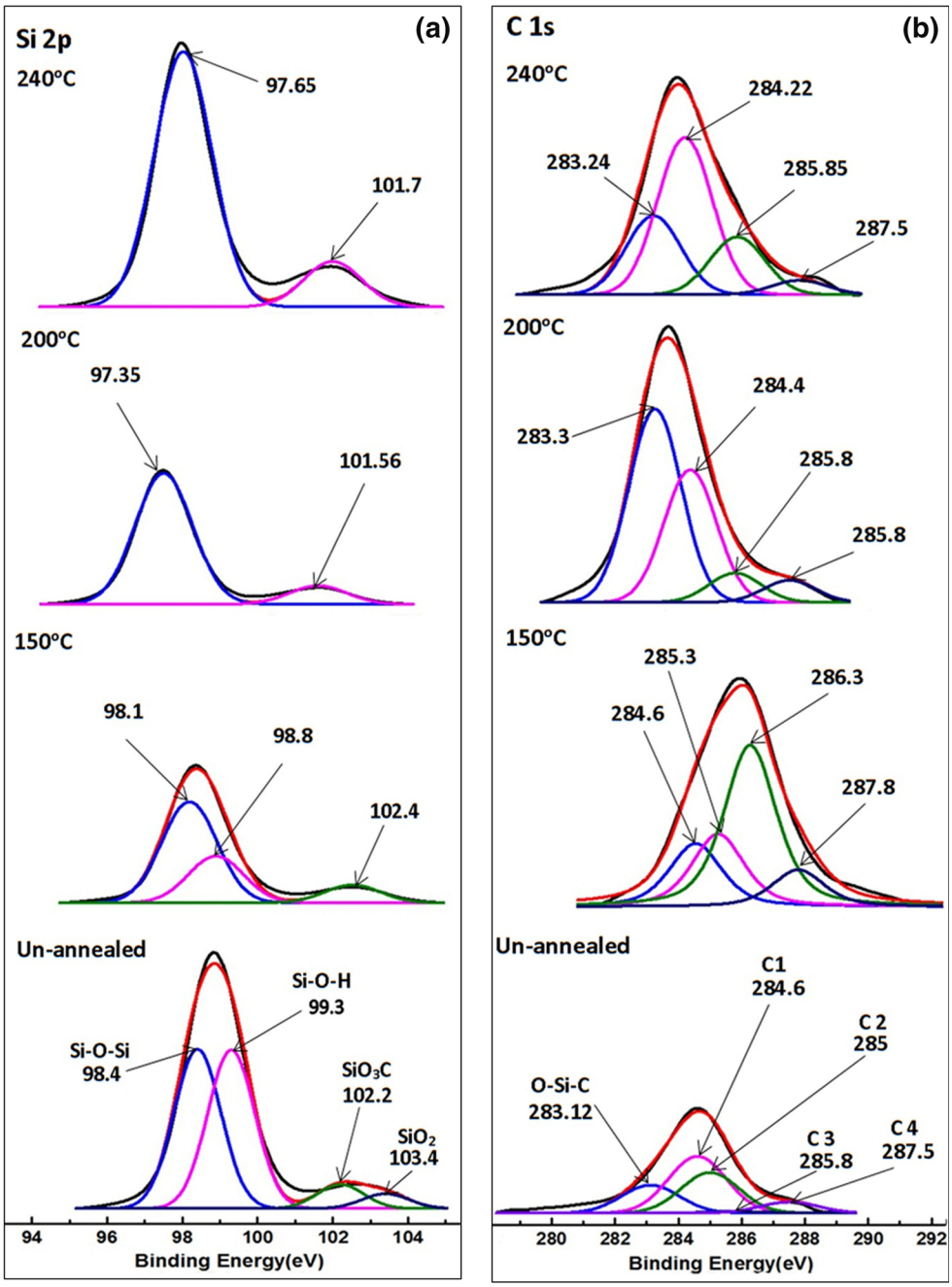

Fig. 3. Deconvoluted XPS spectra of povidone–silicon oxide films annealed at different temperatures. (a) Si2p and (b) C1s electron orbitals.

are no significant differences in the images, but tiny grains are evident in all the samples. According to the study conducted by Yao et al.,[41] this could be attributed to the polymerization process, because, during the condensation process, silicon oxide nanoparticles are formed rapidly but they gradually aggregate. Polymer molecules interact with the primary particles and prevent their aggregation and the emergence of large clusters.[41] In addition, the silane coupling agent plays an important role in the connection between the povidone chains and silicon oxide nanoparticles, leading to homogeneity and a smooth surface.

The values of the average surface roughness (S_a) of 0.037 nm, 0.036 nm, 0.084 nm, and 0.04 nm were obtained for the non-annealed nanocomposite film and the films annealed at 150°C, 200°C, and 240°C, respectively. According to the XPS results, the strongest cross-linking formed between the two phases of the nanocomposite film annealed at 150°C can significantly prevent nanoparticle aggregation and consequently the lowest average

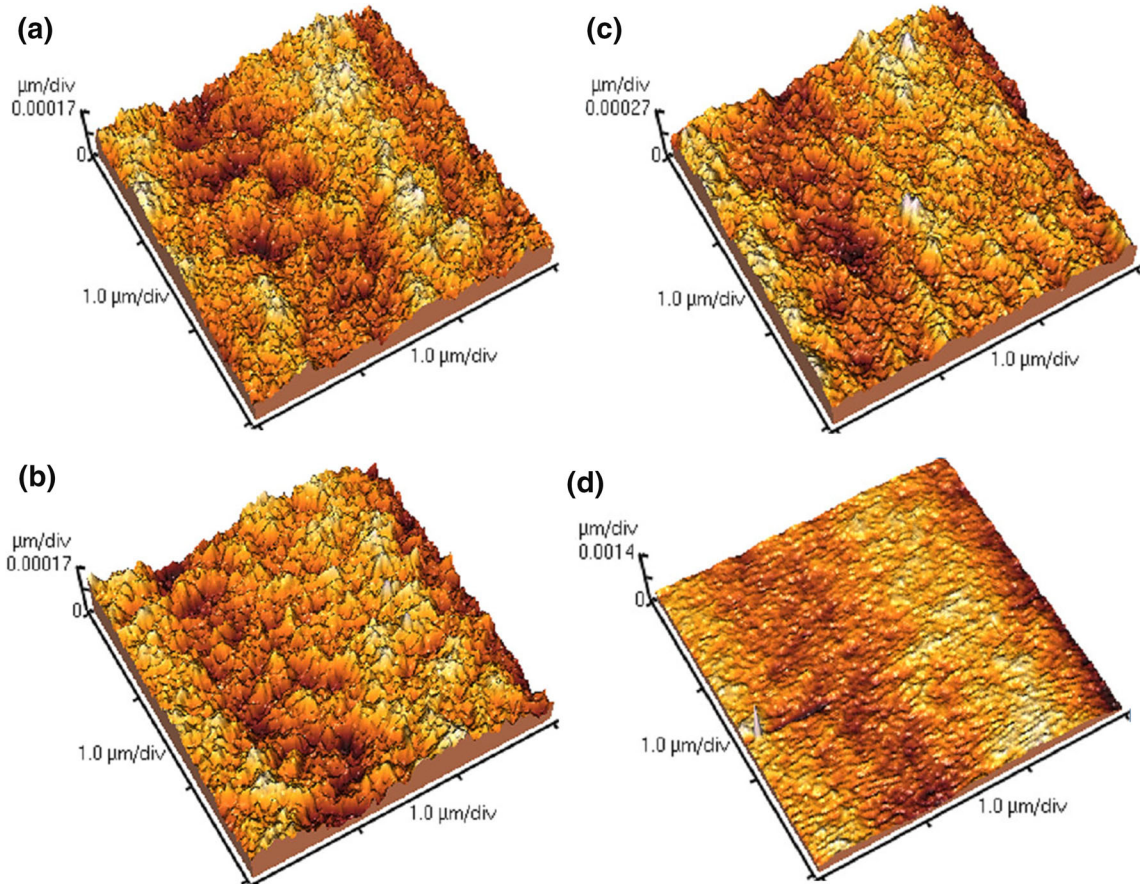

Fig. 4. AFM images of povidone–silicon films (a) not annealed, and annealed at (b) 150°C, (c) 200°C, and (d) 240°C.

Table III. Electrical values of *p*-type silicon FETs based on povidone–silicon oxide nanocomposite gate dielectric films annealed at different temperatures

Sample	C (F/cm^2) × 10^{-8}	V_{th} (V)	μ (Cm^2 V^{-1} s^{-1})	On/off current
Not annealed	1.16	14.5	1.98	3.22×10^4
150°C	1.027	13	3.87	2.32×10^5
200°C	1.278	16	2.27	2.53×10^4
240°C	2.162	17	1.15	2.51×10^4

roughness can resulted. The highest average roughness of the film annealed at 200°C can be attributed to the aggregated structure of the film, as deconvoluted XPS reveals degradation of the Si-O-Si bonds and the appearance of Si-Si and O-Si-C bonds at this temperature. At the highest temperature, many bonds of the nanocomposite film elements were desorbed and aggregation of the film structure decreased. So, compared to the sample annealed at 200°C, a relative decrease in the average roughness was found.

However, all the obtained values of average roughness are significantly low (< 0.084) ,and there are no significant differences between them. The values are much lower than the silicon oxide film,[11] and the values in most of the recent research studies which have investigated inorganic–organic composite dielectric films. For example, the average surface roughness of 0.5 nm,[5] 2.84–43.2 nm[15] and 0.6 nm[29] have been reported for a self-assembled organic layer (SAOL)-ZrO_2, $Ca_2Nb_3O_{10}$ (CNO)-PMMA and PMMA-SiO_2 nanocomposites, respectively. This could be due to the chemical bonds formed between the two phases (according to FTIR and XPS resuts) in the effect of the silane coupling agent which creates cross-linked nanocomposites.

Electrical Studies

The capacitance of povidone–silicon oxide nanocomposite films was determined by capacitance–voltage (C–V) measurements using metal–

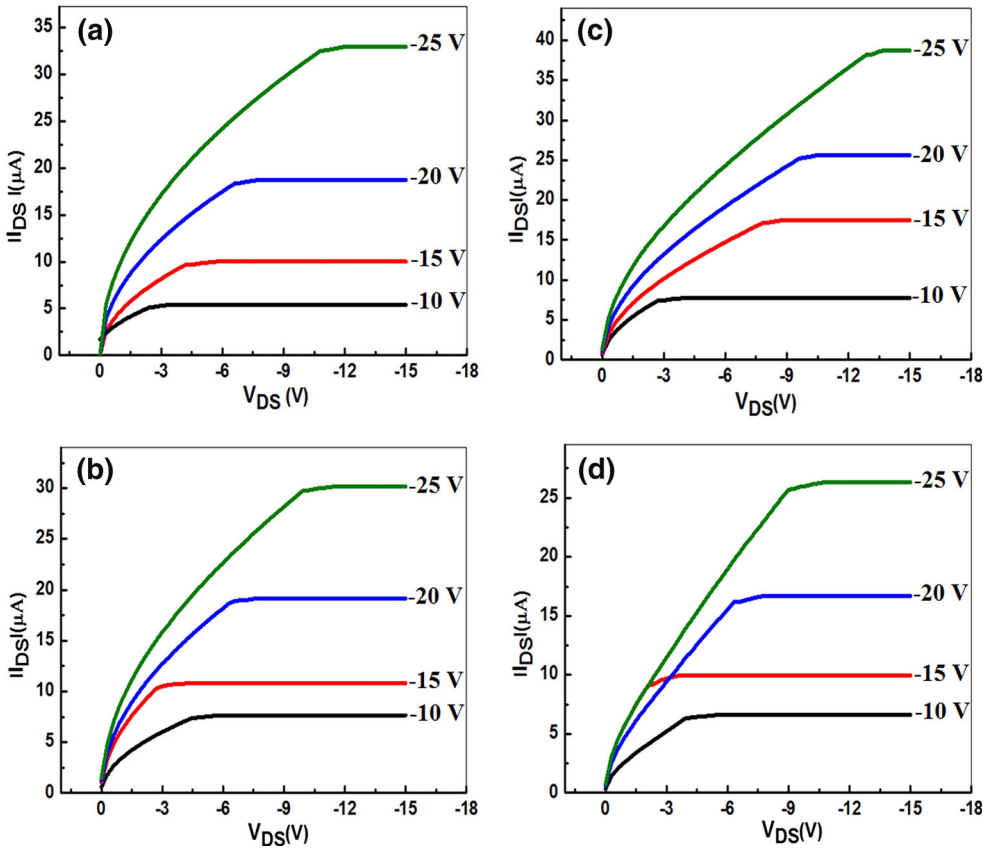

Fig. 5. II_{DS}I versus V_{DS} curves for *p*-type silicon FETS based on nanocomposite dielectric films: (a) not annealed and annealed at (b) 150°C, (c) 200°C, and (d) 240°C, by applying gate voltages from −10 to − 25 V that increase with − 5-V steps.

insulator–semiconductor (MIS) capacitors at room temperature. An Au metal, povidone–silicon oxide nanocomposite and *p*-type silicon (100) were used as the gate, insulator and semiconductor layers, respectively. The C–V measurements were carried out using a Keithley K361 parameter analyzer at room temperature. The average values of capacitance density of the dielectric films obtained from the gate voltages of − 15 to 15 V are listed in Table III.

According to Table III, average capacitances of 1.12×10^{-8} F/cm^2, 1.027×10^{-8} F/cm^2, 1.27×10^{-8} F/cm^2 and 2.16×10^{-8} F/cm^2 have been obtained for the non-annealed nanocomposite films and the films annealed at 150°C, 200°C, and 240°C, respectively. The capacitance of the dielectric film annealed at 150°C reduces in comparison with that of the non-annealed dielectric film. As the annealing temperature increases (200°C and 240°C), the capacitance of the nanocomposite dielectric films increases.

According to the studies conducted by Morales-Acosta et al.,[28,29] "the materials with polar groups have high capacitance due to the orientation of their electrical dipoles in an applied electric field. It is well known that the O-H groups have the highest polarization".[28,29] Therefore, the decreased capacitance of the film annealed at 150°C could be attributed to the formation of a cross-linked nanocomposite structure and decreased Si-OH bonds[8,20,28,29] (see Fig. 3a). In addition, the capacitance of films could have been significantly affected by the chemical structure and defects.[8,18,20,21,28,29,53] The increase in the capacitance of the films annealed at 200°C and 240°C might be related to the degradation of some bonds and the formation of many defects which trap charge carriers.

The electrical characteristics of povidone–silicon oxide nanocomposite films were examined by current–voltage (*I*–*V*) measurements in a MIS structure at room temperature. The MIS device consisted of a povidone–silicon oxide nanocomposite as gate dielectric, the *p*-type silicon (100) as semiconductor and an AU metal as gate electrode (top contact) and source–drain electrodes (top contact). The source and drain electrodes with the channel length and width of 100 μm and 1 mm, respectively, were evaporated on top of the semiconductor *p*-type silicon substrate by a shadow-mask. The photolithography process was used to access the *p*-type silicon substrate. The electrical characteristics of the fabricated *p*-type silicon FETs were measured using a Keithly model K361 parameter analyzer.

Figure 5 displays II_{DS}I versus V_{DS} curves for *p*-type silicon FET*s* by applying a gate voltage of − 10 to − 25 V at − 5-V intervals. Accordingly, all FETs

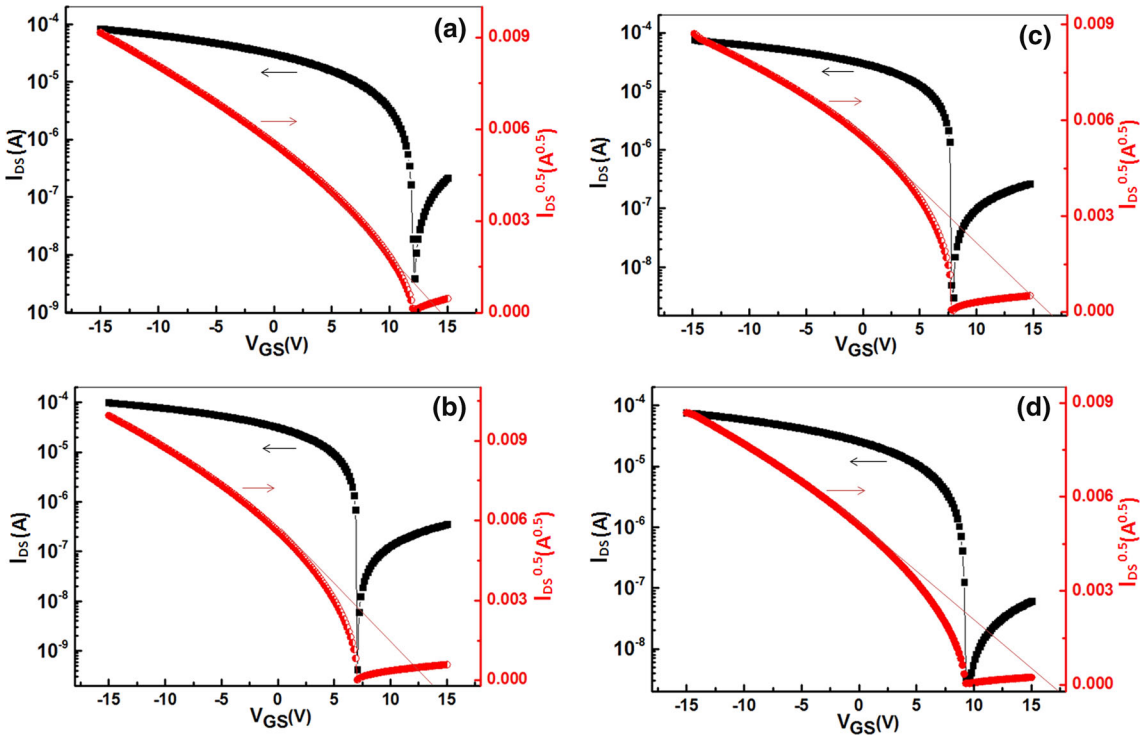

Fig. 6. $I I_{DS} I$ versus V_{GS} curves for *p*-type silicon FETs based on nanocomposite dielectric films: (a) not annealed and annealed at (b) 150°C, (c) 200°C, and (d) 240°C, by applying the gate voltages from − 15 V to 15 V at V_{DS} = −15 V.

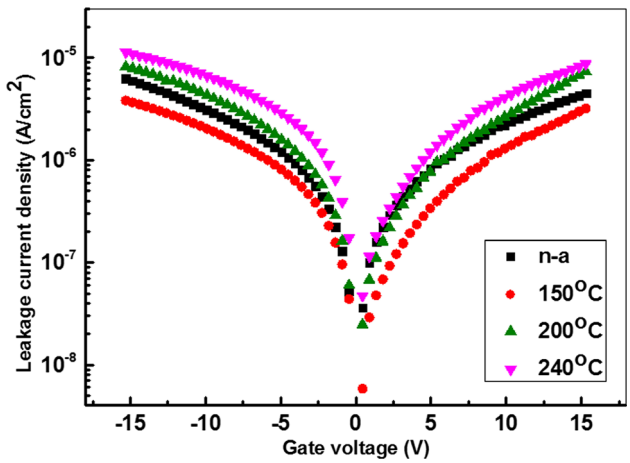

Fig. 7. Gate leakage current density versus gate voltage curves of *p*-type silicon FETs based on nanocomposite dielectric films annealed at different temperatures.

show typical linear and saturation regimes. Figure 6 shows $I I_{DS} I$ versus V_{GS} curvesat a gate voltage of − 15 to 15 V under V_{DS} = − 15 V. The on/off current ratios were extracted from the ratio of maximum to minimum drain current. Threshold voltages (V_{th}) were determined by the intercept of the linear fit from the $I\sqrt{I_{DS}I}$ versus V_{GS} curves. The field effect mobilities (μ) were calculated using the following equation.[42]

$$I_{DS}^{1/2} = \left(\frac{WC_{\mu_{FET}S}}{2L}\right)^{1/2}(V_{GS} - V_{th}) \quad (1)$$

The values of threshold voltage, mobility, on/off ratio and capacitance of all samples are listed in Table III. The fabricated FET based on non-annealed dielectric film shows a field-effect mobility of 1.98 $cm^2\ V^{-1}\ s^{-1}$. The mobility of the FET based on dielectric film annealed at 150°C rises to 3.87 $cm^2\ V^{-1}\ s^{-1}$. A further increase in the annealing temperature leads to the reduction in the mobility compared to FET based on dielectric film annealed at 150°C (2.27 $cm^2\ V^{-1}\ s^{-1}$ and 1.15 $cm^2\ V^{-1}\ s^{-1}$ for FETs based on dielectric films annealed at 200°C and 240°C, respectively). It seems that the motilities have been affected by the nanostructure and interactions of the dielectric film.[8,14,20,28,32,54,55] The highest intensity of Si-OH groups (414.7) which trap the charge carriers in the non-annealed dielectric film could decrease the mobility of the FET.[8,21,28,29,31,47,53] The highest mobility of the FET based on dielectric film annealed at 150°C could be related to the decrease in Si-OH bonds and the formation of a cross-linked structure of the dielectric film, which can improve the nanostructure channel.[8,21,28,31] The disappearance of Si-O-Si bonds which show the degradation of some interactions between dielectric film elements annealed at 200°C with *p*-type silicon

semiconductor film might decrease the mobility of FET compared to the FET fabricated based on dielectric film annealed at 150°C. The disappearance of Si-O-Si bonds and the decrease in Si-O-C bonds, which reflects the degradation of many bonds between the elements of the dielectric film annealed at 240°C, could create more defects in the nanostructure of the channel, resulting in a decrease in the mobility.

However, all values are higher than the hole mobility obtained in some previous studies.[3,5,13,18,43,44] Hole mobilities of 0.02–0.07,[18] 0.2,[3] 0.34,[43] and 1.1[44] have been reported based on PMMA-SiO_2-TMSPM, pentacene, self-assembled monolayer (SAM)-ZnO, and SAM-AlOx gate dielectrics, respectively. According to many research studies,[18,30,33,45–47] one of the factors affecting the mobility is the surface roughness ofthe dielectric film. Hence, this probably relates to the very low surface roughness of nanocomposite films (according to the AFM results).

The threshold voltage of a FET based on the dielectric film annealed at 150°C decreases compared with the one based on non-annealed dielectric film. As the annealing temperatures of the dielectric films increase further (200°C and 240°C), the threshold voltages increase. According to many research studies, V_{th} is affected by the morphology of the dielectric film.[8,18,20,31,32,56–58] The lowest threshold voltage in the FET based on dielectric film annealed at 150°C is probably because of the best adhesion between the dielectric film and the *p*-type silicon semiconductor film (according to the domination of Si-O-Si bonds) and the decrease in hydroxyl groups (as XPS spectra show) which reduces the trapping of charge carriers in the FET channel.[8,14,21,28,29,31]

A similar trend is also observed in the on/off ratios. According to previous studies,[45,46,48] a low value of the on/off current ratio is due to the increase in the leakage current. Figure 7 illustrates gate leakage current density versus gate voltage curves of *p*-type Si FETs, confirming this reason. The leakage current of the FET based on non-annealed dielectric film is in the range of 1.28×10^{-7}–6.26×10^{-6} A/cm^2 for the entire voltage range. The leakage current values of the FET based on dielectric film annealed at 150°C decrease in the range of 1.34×10^{-7}–3.82×10^{-6} A/cm^2 for the entire voltage range. The leakage current values increase as the annealing temperatures go up (2.34×10^{-7}–1.13×10^{-5} A/cm^2 for FET based on dielectric film annealed at 240°C). It is well known that cross-linked dielectric films improve the insulating property.[8,20,21,28,31,46] The strongest cross-linking between the elements of the povidone–silica nanocomposite obtained at 150°C is estimated based on the highest binding energy obtained in XPS spectra causing the lowest leakage current.[8,21,28,31] By increasing the annealing temperature, the interactions of the povidone–silicon oxide dielectric film elements with *p*-type silicon substrate degraded as the Si-O-Si bonds shift toward the lower binding energy in the XPS results. This has created changes in the nanostructure of the nanocomposite and thus gaps might have been created. The charge carriers in the FET channel can diffuse through the gaps of the dielectric film, leading to an increase in gate leakage.[15]However, the leakage current values of all the films are lower than those of the SiO_2 dielectric thin films.[10] Also, these values are low enough to be used as a gate dielectric for Si FETs. This might be related to the formation of strong chemical (hydrogen or covalent bonds) interactions between the elements of the nanocomposite dielectric films.

CONCLUSIONS

In this study, the decreased leakage current densities and the increased mobilities of *p*-type silicon transistors were obtained using a povidone—silicon oxide nanocomposite gate dielectric. The strong hydrogen (Si-OH) and covalent (such as Si-O-Si and Si-O-C) bonds as well as the low surface roughness were created by employing a silane coupling agent and a polar solvent. In addition, it was found that the annealing temperature affects the interaction between the elements of the nanocomposite and the *p*-type silicon semiconductor film. The decrease in the hydrogen bonds and the increase in covalent bonds in the nanocomposite dielectric film annealed at 150°C optimized the merit factors of *p*-type silicon FETs. As the temperature increased (200°C and 240°C), some covalent bonds shifted to a lower binding energy and defects were formed in the nanostructure of the dielectric film, deteriorating the *p*-type silicon FET performance.

REFERENCES

1. B.-R. Wu, T.-H. Tsai, and D.-S. Wuu, *Appl. Surf. Sci.* 354, 216 (2015).
2. A. Srivastava, O. Mangla, and R.K. Nahar, *J. Mater. Sci. Mater. Electron.* 25, 3257 (2014).
3. N. Tripathi, V. Jindal, F. Shahedipour-Sandvik, S. Rajan, and A. Vert, *Solid-State Electron.* 54, 1291 (2010).
4. Z. Khorshidi, A. Bahari, and R. Gholipur, *J. Electron. Mater.* 43, 4349 (2014).
5. B.H. Lee, K.K. Im, K.H. Lee, S. Im, and M.M. Sung, *Thin Solid Films* 517, 4056 (2009).
6. A.Z. Kattamis, R.J. Holmes, I.-C. Cheng, K. Long, J.C. Sturm, S.R. Forrest, and S. Wagner, *J. IEEE Electron Device Lett.* 27, 49 (2006).
7. K.-Y. Chan, J. Kirchhoff, A. Gordijn, D. Knipp, and H. Stiebig, *Thin Solid Films* 517, 6383 (2009).
8. A. Hashemi, A. Bahari, and S. Ghasemi, *Appl. Surf. Sci.* 416, 234 (2017).
9. A. Bahari, M. Roeinfard, and A. Ramzannezhad, *J. Mater. Sci. Electron.* 27, 9363 (2016).
10. H.-W. Lu and J.-G. Hwu, *Appl. Phys. A* 115, 837 (2014).
11. Z. Bao and J. Locklin, *Organic Field-Effect Transistors* (Berlin: Springer, 2007), pp. 341–371.
12. E. Lee, J. Jung, A. Cgoi, X. Bulliard, J.-H. Kim, Y. Yun, J. Kim, J. Park, S. Lee, and Y. Kang, *RSC Adv.* 7, 17841 (2017).
13. T. Umeda, D. Kumaki, and S. Tokito, *Org. Electron.* 9, 545 (2008).

14. S. Faraji, T. Hashimoto, M.L. Turner, and L. Majewski, *Org. Electron.* 17, 178 (2015).
15. X. Wu, F. Fei, Z. Chen, W. Su, and Z. Cui, *Compos. Sci. Technol.* 94, 117 (2014).
16. K. Takagi, T. Nagase, T. Kobayashi, and H. Naito, *Org. Electron.* 32, 65 (2016).
17. M. Makrygianni, A. Ainsebaa, M. Nagel, S. Sanaur, Y.S. Raptis, I. Zergioti, and D. Tsamaki, *Appl. Surf. Sci.* 390, 823 (2016).
18. M. Shahbazi, A. Bahari, and S. Ghasemi, *Synth. Met.* 221, 332 (2016).
19. V.R. Reddy, *J. Appl. Phys. A.* 116, 1379 (2014).
20. F.-Y. Yang, K.-J. Chang, M.-Y. Hsu, and C.-C. Liu, *J. Mater. Chem.* 18, 5927 (2008).
21. S.H. Kim, S.Y. Yang, W. Shin, H. Jeon, J.W. Lee, K.P. Hong, and C.E. Park, *Appl. Phys. Lett.* 89, 183516 (2006).
22. S. Faraji, E. Danesh, D. Julate, and M.L. Yurner, *Appl. Phys.* 49, 185102 (2016).
23. M. Shahbazi, A. Bahari, and S. Ghasem, *Org. Electron.* 32, 100 (2016).
24. H. Najafi-Ashtiani, A. Bahari, and S. Ghasemi, *Org. Electron.* 37, 213 (2016).
25. H. Najafi-Ashtiani and A. Bahari, *Synth. Met.* 217, 19 (2016).
26. R. Gholipur and A. Bahari, *Appl. Phys. A* 122, 536 (2016).
27. A. Hashemi and A. Bahari, S, Ghasemi. *J. Mater. Sci. Mater. Electron.* 28, 13313 (2017).
28. M.D. Morales-Acosta, C.G. Alvarado-Beltran, M.A. Quevedo-Lopez, and B.E. Gnade, *J. Non-Cryst. Solids* 362, 124 (2013).
29. M.D. Morales-Acosta, M.A. Quevedo-Lopez, B.E. Gnade, and R. Ramirez-Bon, *J. Sol-Gel. Sci. Technol.* 58, 218 (2011).
30. L.S. Cardoso, J.C. Stefanelo, and R.M. Faria, *Synth. Met.* 220, 286 (2016).
31. C.-M. Keum, J.-H. Bae, M.-H. Kim, W. Choi, and S.-D. Lee, *Org. Electron.* 13, 778 (2012).
32. S. Kim, A. Kim, K.-S. Jang, S. Yoo, J.-W. Ka, J. Kim, M.H. Yi, J.C. Won, S.-K. Hong, and Y.H. Kim, *Synth. Met.* 220, 311 (2016).
33. Michael A. Derenge, K.W. Kirchner, K.A. Jones, P. Suvarna, and S. Shahedipour-Sandvik, *J. Solid-State Electron.* 101, 23 (2014).
34. A. Hashemi and A. Bahari, *Appl. Phys. A* 123, 535 (2017).
35. B. Gao and Z. Wang, *J. Colloid Surf. B. Biointerfaces* 79, 446 (2010).
36. B. Arkles, *Silane Coupling Agent* (Morrisville: Gelest. Inc, 2006), pp. 2–12.
37. F. Jolly, F. Rochet, G. Dufour, C. Grupp, and A. Table-Ibrahimi, *J. Non-Cryst. Solids* 280, 150 (2001).
38. K.V. Egorov, Y.Y. Lebedinskii, A.M. Markeeva, and O.M. Orlov, *Appl. Surf. Sci.* 356, 454 (2015).
39. V. Thakur and S.M. Shivaprasad, *Appl. Surf. Sci.* 327, 389 (2015).
40. A.G. Silva, K. Pedersen, Z.S. Li, and P. Morgen, *Appl. Surf. Sci.* 353, 1208 (2015).
41. Y. Xu and D. Wu, *J. Colloid Surf. A Physicochem.* 305, 97 (2007).
42. I. Karteri, S. Karatas, and F. Yakuphano, *Appl. Surf. Sci.* 318, 74 (2014).
43. C. Yang, Y. Kwack, S.H. Kim, T.K. An, K. Hong, S. Nam, M. Park, W.-S. Choi, and C.E. Park, *Org. Electron.* 12, 411 (2011).
44. D.O. Hutchins, O. Acton, T. Weidner, N. Cernetic, J.E. Baio, D.G. Castner, and H. Ma, A. K-Y. Jen. *Appl. Surf. Sci.* 261, 908 (2012).
45. R.P. Tompkins, I. Mahaboob, S. Shahedipour-sandvik, and N. Lazarus, *J. Adv. Electrochem. Sci. Technol.* 72, 89 (2016).
46. X. Fang, C. Lin, Y. Sun, H. Chin, H.-W. Zan, H.-F. Meng, S.-F. Horng, and L.A. Wang, *Org. Electron.* 31, 227 (2016).
47. P. Kim, X.-H. Zhang, B. Domercq, S.C. Jones, and P.J. Hotchkiss, *Appl. Phys. Letter* 93, 013302 (2008).
48. J. Zhang, H. Zhu, and L. Zhang, *Org. Electron.* 13, 733 (2012).
49. R. Navamathavan, C.Y. Kim, and A.S. Jung, *J. Korean Phys. Soc.* 53, 351 (2008).
50. A. Bahari, *J. Nanostruct.* 1, 54 (2012).
51. H.T. Oyama and J.P. Wightman, *J. Surf. Interface Anal.* 26, 39 (1998).
52. T. Watanabe, S. Hasegawa, N. Wakiyama, F. Usui, A. Kusai, T. Isobe, and M. Senna, *J. Solid State Chem.* 164, 27 (2002).
53. M. Shahbazi, A. Bahari, and S. Ghasemi, *Organ. Electron* 32, 100 (2016).
54. T.T. Dao and M.H. Murata, *IEICE Trans. Electron.* E98-c, 422 (2015).
55. S. Faraji, E. Danesh, D.J. Tate, M.L. Turner, and L.A. Majewski, *J. Phys. D Appl. Phys.* 49, 185102 (2016).
56. W. Ye, J. Deng, X. Wang, and L. Cui, *Appl. Surf. Sci.* 390, 831 (2016).
57. H.X. Xu, J.P. Xu, C.X. Li, C.L. Chan, and P. T. Lai. *Appl. Phys. A* 99, 903 (2010).
58. M.-K, Lee, C.-F, Yen, and C.-H, Fan, *Appl. Phys. A* 116, 2007 (2014).